SYNTHESIS, CHARACTERIZATION AND ANTI-MICROBIAL ACTIVITY OF THIOPHENE-2,5- DICARBOXYLIC ACID AND NEUTRAL HYDRAZINE MIXED LIGAND COMPLEXES OF DIVALENT TRANSITION METALS

[1] Kartik Pundir, [2]Dr. Shiv Brat Singh
[1]Research Scholar, [2]Supervisor
[1-2] Department of Chemistry, CMJ University, Meghalaya, India

Abstract

This study focuses on the synthesis, characterization, and antimicrobial activity of novel thiophene-2,5-dicarboxylic acid (Tdc) and hydrazine mixed-ligand complexes of divalent transition metals (Co^{2+}, Ni^{2+}, Cu^{2+}, Mn^{2+}, Zn^{2+}). These complexes were synthesized by reacting thiophene-2,5-dicarboxylic acid with hydrazine in the presence of metal salts, leading to the formation of $M(Tdc)(N_2H_4)_4$ for Co^{2+}, Ni^{2+}, Zn^{2+} and $M(Tdc)(N_2H_4)_2$ for Cu^{2+} and Mn^{2+}. The structures of the complexes were confirmed through various techniques, including FT-IR, Raman, XRD, TG-DTA, EPR, and antimicrobial testing. The results show that these complexes exhibit significant antimicrobial activity against bacterial strains such as *Pseudomonas vulgaris*, *Staphylococcus aureus*, and *Escherichia coli*, with some complexes surpassing the efficacy of conventional antibiotics like Streptomycin. These findings suggest their potential as promising antimicrobial agents for therapeutic applications.

Keywords: Hydrazine, Thiophene-2,5-dicarboxylate, Transition metals, Antimicrobial activity, Coordination chemistry, EPR spectroscopy

1. Introduction

In the last 50 years much amount of work has been done world wide on the coordination compounds of diamines where H2N-NH2 (hydrazine) is the basic component. Hydrazine is a versatile ligand and it contracts the chance of different modes of coordination to transition metal ions, viz., as a monodentate or bridging bidentate ligand.[1–7] The neutral hydrazine carboxylates of the transition metal ions with diversity of carboxylic acids, including simple aliphatic mono carboxylic acids,[8,9] aliphatic dicarboxylic acids,[10–14] aromatic mono- and dicarboxylic acids,[15,16] heterocyclic acids[17,18] and some aliphatic and aromatic polycarboxylic acids[19–21] have been reported. Thermal degradation studies on hydrazine containing metal carboxylates are of more attention than their non-carboxylate complements due to their easier combustibility to produce fine particles of the metal carbonates or metal oxides.[22–24] The growing interest in hydrazine chemistry has been largely driven by the synthesis, characterization, and biological activity of metal complexes involving sulfur-containing thiophene dicarboxylic acids, which possess a variety of intriguing properties. Among these, thiophene-2,5-dicarboxylate (Tdc^{2-}) anions are particularly noteworthy due to their ability to exhibit multiple coordination modes, including monodentate, bidentate, tridentate, and tetradentate. These diverse coordination behaviors of thiophene-2,5-dicarboxylic acid (H_2tdc) with metal ions are illustrated in Figure 1. Recent studies have focused on the preparation and characterization of novel copper(II) thiophene-2,5-dicarboxylate (tdc) complexes, which are coordinated with various amines such as N-methylethylenediamine, N,N-dimethylethylenediamine, N,N'-dimethylethylenediamine, N,N,N',N'-tetramethylethylenediamine, N-ethylethylenediamine, and N,N'-diethylethylenediamine. Additionally, several zinc(II), cobalt(II), and manganese(II) coordination complexes, including [Zn(Tdc)(py)]n, [Zn(Tdc)(bipy)(H_2O)·1.5H_2O]n, [Zn(Tdc)(phen)(H_2O)]n, [Co(Tdc)(phen)(H_2O)]n, [Mn(Tdc)(phen)]n, and [Mn(Tdc)(H_2O)$_2$]n, have been synthesized and structurally characterized, demonstrating the versatility of thiophene-2,5-dicarboxylate in metal coordination chemistry.

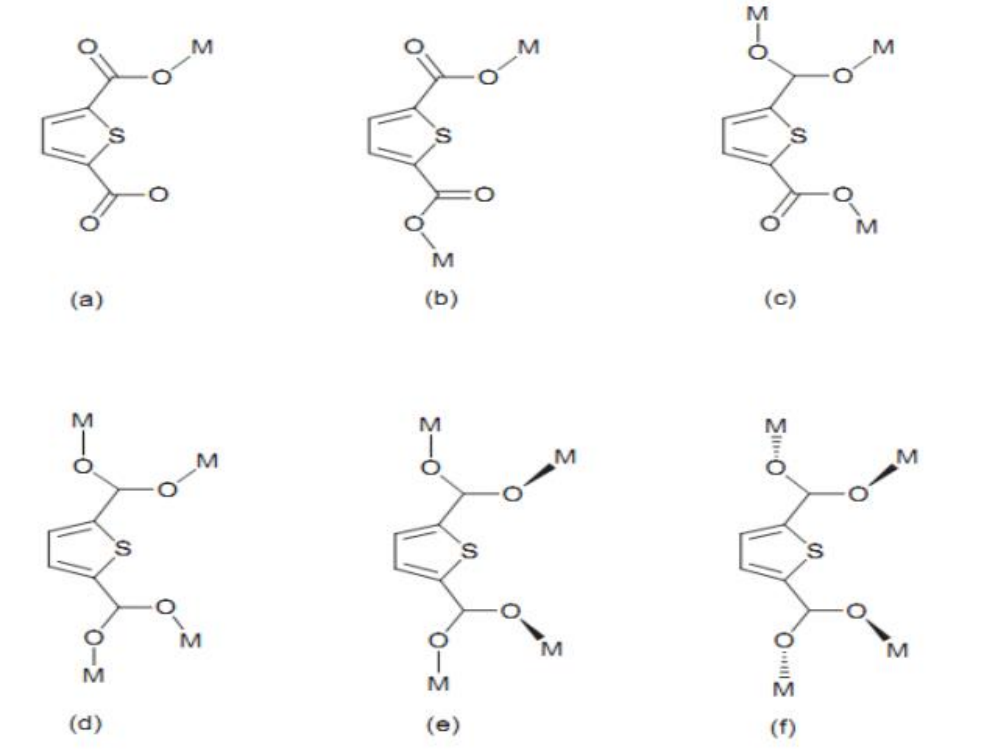

Fig. 1. Various coordination modes of Tdc2– in its metal complexes.

Thorough examination of the literature reveal that the explorations on the biologically significant transition metal complexes featuring thiophene-2,5-dicarboxylic acid and hydrazine as combined–ligands have not been documented thus far. In this endeavour, the amalgamate, portrayal, thermic investigations, and antimicrobial efficacy of several novel bivalent transition metal (Cobalt, Manganese, Copper, Nickel, and Zinc) compounds of thiophene -2,5-dicarboxylic acid with uncharged hydrazine as an accompanying ligand has been expounded.

2. Experimental section

2.1 Materials and methods

Elaborations regarding the substances and various physico-chemical techniques utilised in this study (Analytical, ESI-mass, electronic, FT-IR, Raman and EPR spectroscopic, powder X-ray diffraction, TG–DTA, SEM and antimicrobial properties) are elucidated in Chapter II.

2.2 Synthesis of M(Tdc)(N2H4)n, where n=4 for M=Co, Ni and Zn; and n=2 for M=Cu and Mn

Thiophene-2,5-dicarboxylic acid (0.689 g, 0.004 mol) was introduced to 50 mL of dual purified water containing 0.195 mL (0.004 mol) of unadulterated (99.5%) hydrazine hydrate. The amalgamation solution was agitated thoroughly incessantly and warmed over aqueous bath at 90 °C to obtain lucid solution with acidity 5. This ligand solution was poured softly to an aqueous solution containing 0.004 mol of the corresponding metal nitrate hexahydrate (e.g. 1.19 g of Zn(NO3)2.6H2O, 0.004 mol) with continuous stirring and the solution was then concentrated to one fourth of its volume by heating over boiling water bath at 80–90 °C. When this concentrated solution was permitted to cool at ambient temperature for one day, the multiphase powder compound was entirely preci pitated. It was strained using G4 porous crucible and rinsed with dual distilled water, ethanol and hydrocarbon and ultimately dehydrated in heated air oven. In the instance of copper and manganese compounds, Cu(NO3)2·3H2O and manganese(II) acetate tetrahydrate (Mn(CH3COO)2·4H2O) were employed, pursuing the identical pathway.

3. Results and Discussion

3.1 Elemental and mass spectral analysis

The watery solutions of thiophene-2,5-dicarboxylic acid and hydrazine hydrate interact with watery solution of metal nitrates (or) metal acetate to generate complexes as provided below:

$$M(NO_3)_2{\cdot}6H_2O + C_4H_2S(COOH)_2 + 4N_2H_4{\cdot}H_2O \rightarrow$$

$$[M(C_4H_2S(COO)_2(N_2H_4)_4] + 2HNO_3 + 10H_2O \rightarrow \textbf{(1)}$$

where M = Co, Ni and Zn

$$Cu(NO_3)_2{\cdot}3H_2O + C_4H_2S(COOH)_2 + 2N_2H_4{\cdot}H_2O \rightarrow$$

$$[Cu(C_4H_2S(COO)_2(N_2H_4)_2] + 2HNO_3 + 5H_2O \rightarrow \textbf{(2)}$$

$$Mn(CH_3COO)_2{\cdot}4H_2O + C_4H_2S(COOH)_2 + 2N_2H_4{\cdot}H_2O \rightarrow$$

$$[Mn(C_4H_2S(COO)_2(N_2H_4)_2] + 2CH_3COOH + 6H_2O \rightarrow \textbf{(3)}$$

The experimental synthesis of hydrazine metal complexes revealed that all synthesized compounds were insoluble in water and common organic solvents, indicating unique molecular structures and intermolecular interactions. This insolubility may stem from specific functional groups or coordination geometries that prevent stable solvation around the metal ions. However, the complexes showed limited solubility in a methanol-acetylacetone mixture, especially at elevated temperatures. Notably, they remained stable under atmospheric conditions. Elemental analysis, along with hydrazine and metal content data (Table 1), provided insights into their compositions, essential for understanding their properties. Mass spectra of Co(II), Ni(II), and Cu(II) complexes (Figure 2) showed molecular ion peaks at m/z 378.97 (m+Na)+, 376.03 (m+NH4)+, and 301.95 (m+2H)+, correlating with their formula weights, confirming the reliability of the data. The molecular formulas were determined as $Co(Tdc)(N_2H_4)_4$, $Ni(Tdc)(N_2H_4)_4$, $Cu(Tdc)(N_2H_4)_2$, $Mn(Tdc)(N_2H_4)_2$, and $Zn(Tdc)(N_2H_4)_4$.

Table 1 Analytical data

Compound (Colour)	Molecular mass	Proposed molecular formula	Weight % – Found (calculated)					
			Carbon (CHNS)	Hydrogen (CHNS)	Nitrogen (CHNS)	Sulfur (CHNS)	Metal (ICP-OES)	Hydrazine
Mn(Tdc)(N2H4)2 (yellow)	289.18	MnC6H10O4N4S	21(28)	3.1(3.4)	19.9(19.3)	11.5(11.0)	18.4(18.9)	22.5(22.1)
Co(Tdc)(N2H4)4 (light red)	357.25	CoC6H18O4N8S	20.6(20.1)	5.2(5.0)	30.8(31.3)	8.2(8.9)	16.1(16.4)	35.2(35.8)
Ni(Tdc)(N2H4)4 (pale blue)	357.01	NiC6H18O4N8S	20.7(20.1)	9(5.0)	31.1(31.3)	8.4(8.9)	16.6(16.4)	35.3(35.8)
Cu(Tdc)(N2H4)2 (green)	297.79	CuC6H10O4N4S	23.5(21)	3.0(3.3)	18.3(18.8)	10.0(10.7)	20.8(21.3)	21.1(21.5)
Zn(Tdc)(N2H4)	363.73	ZnC6H18O4N8S	19.2(19.7)	2(9)	30.2(30.7)	8.2(8.8)	18.2(17.9)	39(35.2)

4 (dirty white)								

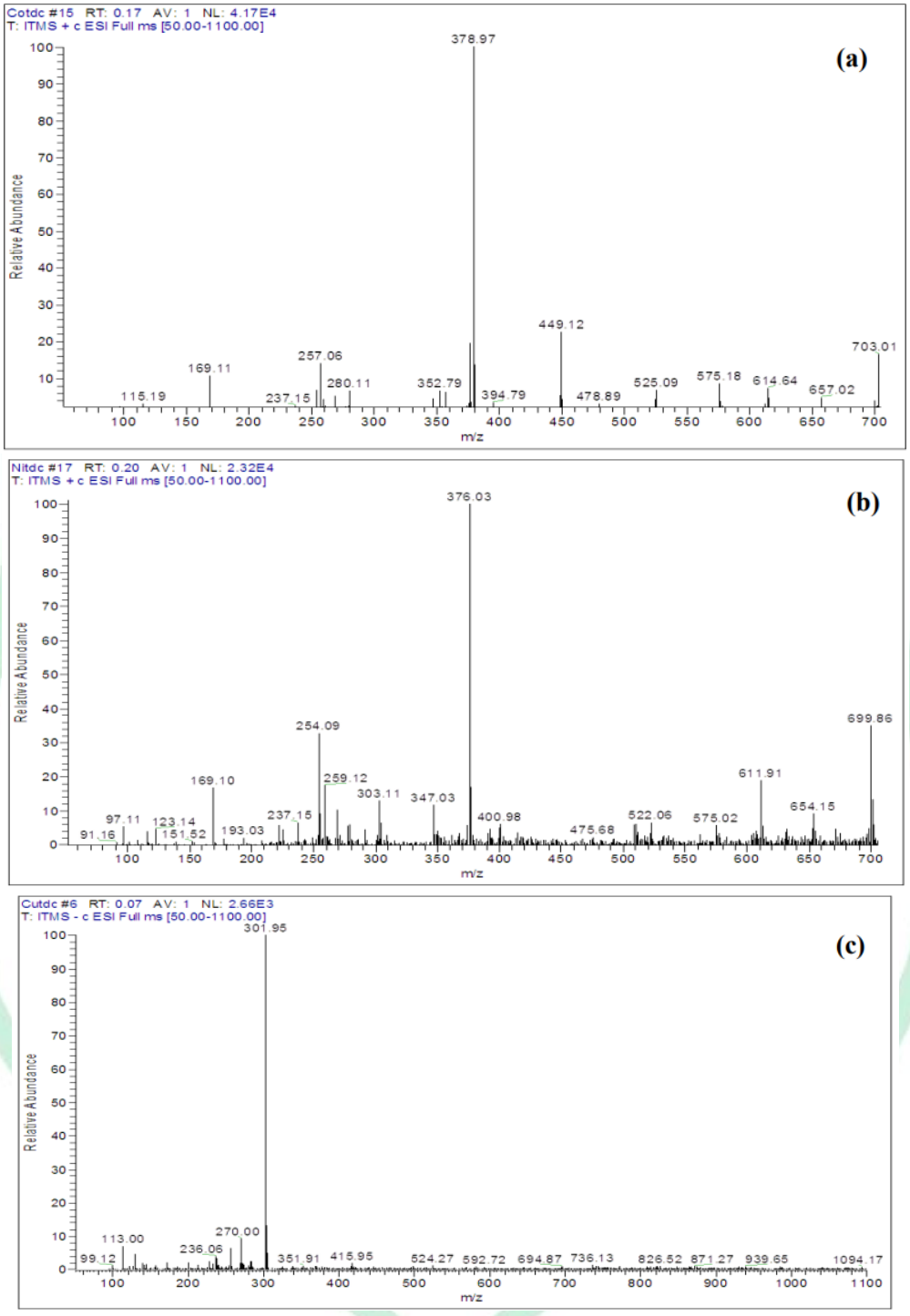

Fig. 2. Mass spectra of (a) Co(Tdc)(N2H4)4, (b) Ni(Tdc)(N2H4)4 and (c) Cu(Tdc)(N2H4)2.

3.2 Infrared and Raman spectra

The FTIR and Raman frequencies of the synthesized complexes are summarized in Table 2, with FTIR spectra shown

in Figure 3. All complexes display strong absorption bands in the 3200–3300 cm–1 range, corresponding to N–H stretching of the hydrazine molecule. The carboxylate ion stretching vibrations appear at 1614–1675 cm–1 and 1372–1400 cm–1, with a Δ ~250 cm–1 difference, indicating unidentate coordination of both carboxylate groups. N–N stretching frequencies for Co, Ni, Cu, and Zn complexes are in the 931–934 cm–1 range, suggesting monodentate hydrazine coordination, while the Mn(II) complex shows N–N stretching at 963 cm–1, indicating bidentate coordination. Additionally, the presence of M–O bands at 537–569 cm–1 and M–N bands at 463–481 cm–1 further supports the coordination of the hydrazine and carboxylate groups.

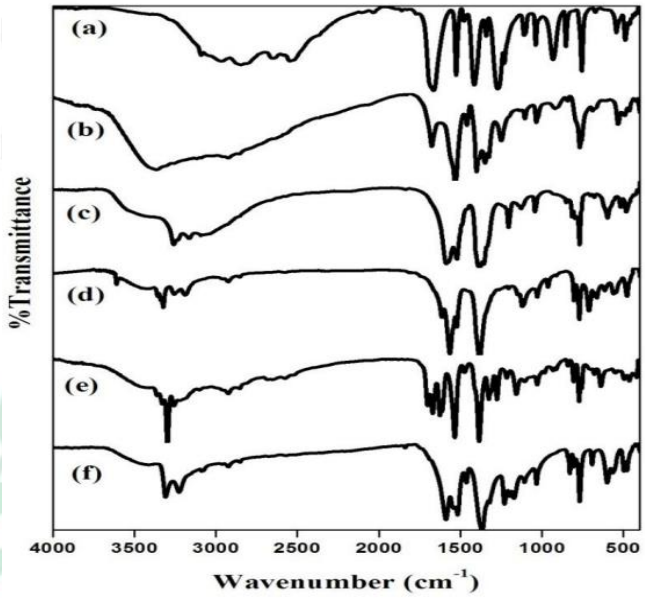

Fig. 3. FTIR Spectra of thiophene-2,5-dicarboxylic acid (a); [Co(Tdc)(N2H4)4] (b); [Cu(Tdc)(N2H4)2] (c); [Mn(Tdc)(N2H4)2] (d); [Ni(Tdc)(N2H4)4] (e); [Zn(Tdc)(N2H4)4](f).

The Raman spectra witnessed for the metal thiophene-2,5-dicarboxylates and thiophene-2,5-dicarboxylic acid are displayed in Fig. The Raman spectrum of thiophene-2,5-dicarboxylic acid displays the distinctive peak of the carbonyl group: (C=O) 1688 cm–1, off-axis flexing oscillations of the carboxylic group: γ(OH)COOH 927 cm–1, and the elongation oscillation of the hydroxyl group (OH)COOH 3087 cm–1. The spectrums of metal complexes do not display the distinctive bands caused by COOH flexing or elongating, which demonstrated that the carboxylate groups are engaged in the coordination with the metal ion. Substitution of the carboxylic group hydrogen with a metallic ion induces a modification in the bond intensities of carboxylate groups and thus exhibits carboxylate elongation oscillations at reduced frequencies compared to those detected for the ligand. Hence, in the spectra of complexes, the bands designated to carboxylic group oscillations vanished, and peaks derived from carboxylate anion oscillation transpired. The ensemble perceived in the vicinity of 1524–1562 cm–1 is attributable to the elongation oscillations of the fragrant circle, which manifested at approximately a comparable spectrum of wavenumbers both in the ligand and in the metallic compounds. This implies that the fragrant system is not disrupted significantly upon coordination of thiophene-2,5-dicarboxylic acid with metals via carboxylate groups. A group acquired within the span of 1118–1136 cm–1 signifies the elongation oscillation of the fragrant carbon-sulfur sequence (C-S)ar.

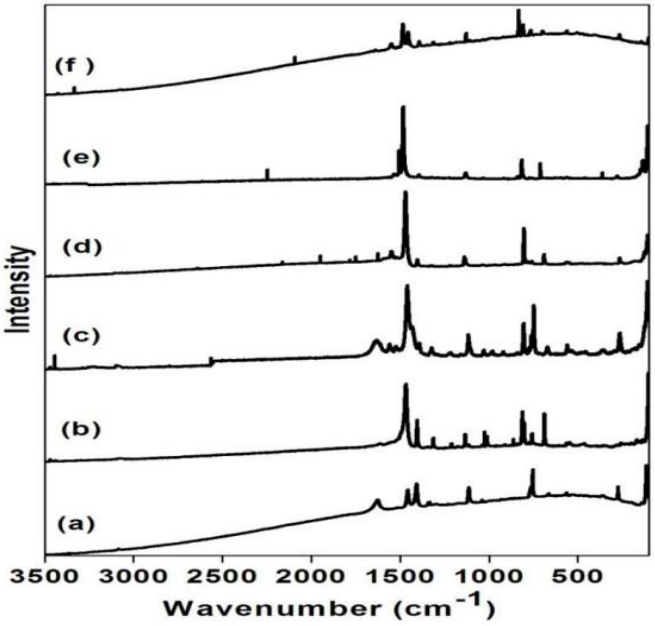

Fig. Raman spectra of thiophene-2,5-dicarboxylic acid (a) and complexes of cobalt (b), nickel (c), manganese (d), copper (e) and zinc (f) carboxylates.

Table 2 FTIR and Raman spectral data (cm–1)

(Assignments of selected bands (cm–1) observed in the IR and Raman spectra of thiophene-2,5-dicarboxylic acid and cobalt(II), nickel(II), manganese(II), copper(II) and zinc(II) thiophene-2, 5-dicarboxylates (complexes).)

H2Tdc		**Co(Tdc)(N2H4)4**		**Ni(Tdc)(N2H4)4**		**Mn(Tdc)(N2H4)2**		**Cu(Tdc)(N2H4)2**		Zn(Tdc)(N2H4)4		Assignment
IR	Raman	IR	Raman	IR	Raman	IR	Raman	IR	Raman	IR	Raman	
3083 vw	3087 w	–	–	–	–	–	–	–	–	–	–	(OH)COOH
1684 s	1688 m	–	–	–	–	–	–	–	–	–	–	(C=O)
–	–	1675 vs	1678vw	1625 vs	1631 s	1614 m	1631 m	1624 vs	–	1630 vs	1644 m	– as(COO)
1525 vs	–	1533 vs	–	1535 vs	1524 m	1564 vs	1549 s	1546 vs	1537 w	1577 vs	1562 s	(CC)ar
–	–	1400 vs	1403 s	1384 vs	1393 w	1382 vs	1406 m	1372 vs	1393 w	1378 vs	1393 s	– s(COO)
1109 s	1112 s	1105 m	1114 m	1105 m	1111 s	1119 s	1125 w	1109 s	1103 w	1107 s	1105 m	(C-S)ar
–	–	934 w	910 w	934 w	921 w	963 w	965 w	931 w	917 w	933 w	919 w	(N–N)
925 vs	927 vw	–	–	–	–	–	–	–	–	–	–	γ(OH)COOH
–	–	543 m	546 m	556 m	560 m	569 m	566 m	537 m	558 m	563 m	561 m	–O)
–	–	463 m	463 s	463 m	457 s	481 m	479 s	463 m	459 w	472 m	472 m	(M–N)

3.3 Electronic and EPR spectra

The digital spectra of Cobalt(Tdc)(N2H4)4, Nickel(Tdc)(N2H4)4 and Copper(Tdc)(N2H4)2 are provided in Figure 5. The assimilation spectrum of independent ligand (thiophene-2,5-dicarboxylic acid) consist of a strong band detected at 289 nm, which is attributed to n–π* shifts of the carbonyl cluster (C=O). These changes are likewise noticed in the spectra of all the compounds, but they moved towards reduced frequencies (~275 nm) in comparison to that of the independent ligand (289), validating the binding of the ligand to the metal ions. The electromagnetic spectrum of the cobalt compound exhibited a robust band within the 15,384–23,529 cm–1 (425–650 nm) interval, which is attributed to the distinctive 4T1g (F) → 4T1g (P) shift of the six coordinated cobalt(II) complex.32 The Ni(II) compound displayed a robust band in the range of 14,825–22,222 cm–1 (450–700 nm) attributed to 3A2g → 3T1g (P) shift distinctive of octahedral structure. In the instance of Cu(II) compound, a band emerged approximately 13,333–19,047 cm–1 (525–750 nm). This alteration is emblematic of quadrilateral planar surroundings around Cu(II) metal ion and the alteration is designated as 2B1g → 2Eg alteration.

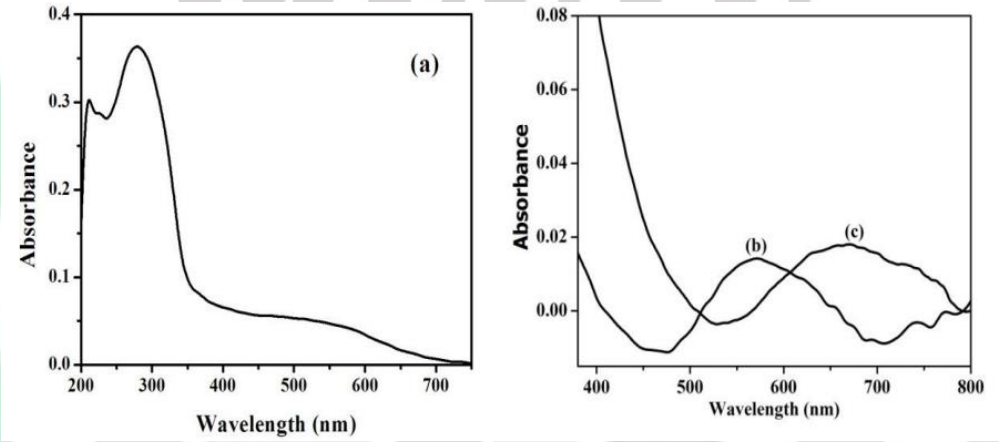

Fig. 5. Electronic Spectra of (a) Co(Tdc)(N2H4)4; (b) Ni(Tdc)(N2H4)4; (c) Cu(Tdc)(N2H4)2.

The EPR spectra of the cobalt(II), nickel(II), copper(II), and manganese(II) compounds (solid samples) at ambient temperature are shown in Figure 6. The spectra reveal axial symmetry with g∥ and g⊥ values, determined using DPPH as a reference, listed in Table 3. No hyperfine splitting was observed, indicating the paramagnetic center is undiluted. For the Cu(II) complex, g∥ (2.213) is greater than g⊥ (2.176), suggesting that the unpaired electron is in the dx2–y2 orbital, typical of a distorted square planar geometry. Based on Kivelson and Neiman's criteria, the g values indicate a covalent metal–ligand bond. For Cu(II), g > 2.04 and G < 4 suggest an elongated square-coplanar structure with notable exchange interaction. In contrast, the Co(II) and Ni(II) complexes, with g values < 2.03, suggest an axially compressed octahedral geometry with no exchange interaction.

Table 3 EPR spectral data of the prepared complexes

Complex	g∥	g⊥	giso
Mn(Tdc)(N2H4)2	–	–	2.082
Ni(Tdc)(N2H4)4	2.221	1.855	1.977
Cu(Tdc)(N2H4)2	2.213	2.176	2.188
Co(Tdc)(N2H4)4	2.156	2.024	2.068

$$g_{iso} = g_{\parallel} + 2g_{\perp}/3$$

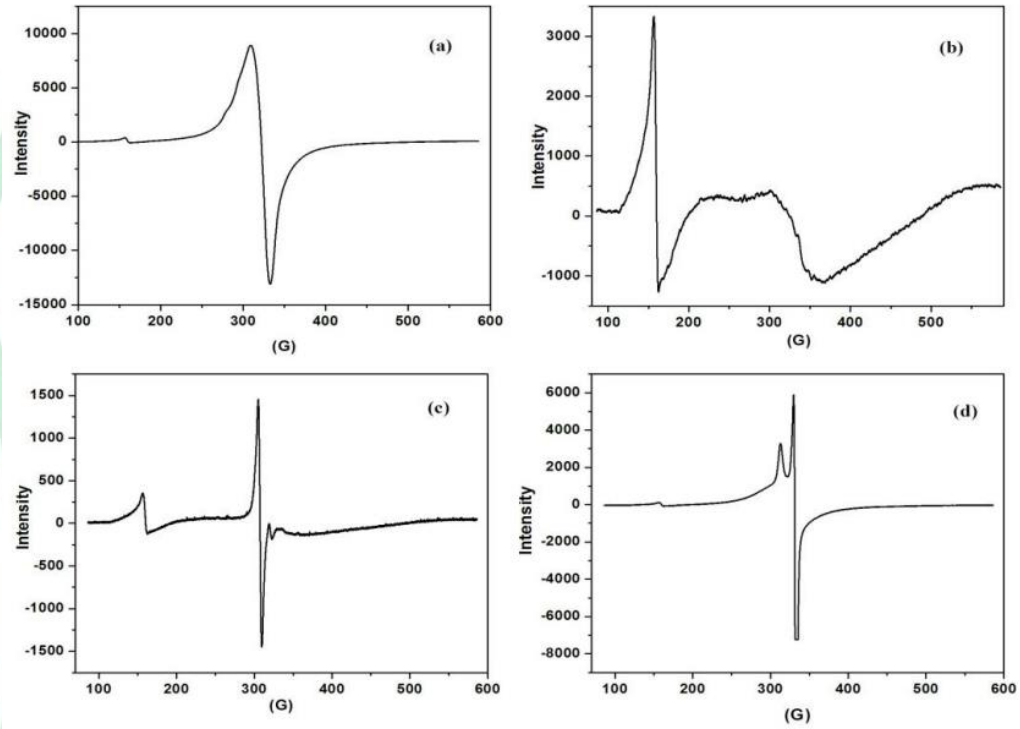

Fig. 6. EPR spectra of (a) Mn(II), (b) Ni(II), (c) Cu(II) and (d) Co(II) Complexes at RT.

3.4 Thermal analysis

The concurrent TG–DTA curves acquired for Cobalt(II), Manganese(II), Nickel(II), Copper(II), and Zinc(II) complexes are depicted in Figure 7, while the thermal examination information is provided in Table The mass depletions of the assemblages of Cobalt and Copper occur in three stages. In the preliminary two stages (110–150 °C and 250–300 °C) dehydration of the compound occurs thermally to yield the corresponding metal thiophene-2,5-dicarboxylate as an intermediary. These intermediaries on additional reduction of organic substance exothermically at approximately 360 °C to produce the metallic oxide as ultimate remainder. The thermic disintegration of Mn(II), Ni(II) and Zn(II) compounds transpires in a solitary phase endoergic shift at approximately 370, 280 and 350 °C correspondingly, and the ultimate deposit is metallic oxide. The compounds of Mn and Ni disintegrate thermally by concurrent dehydrazination and oxidation of the organic substance to yield the corresponding metal oxide as an ultimate outcome.

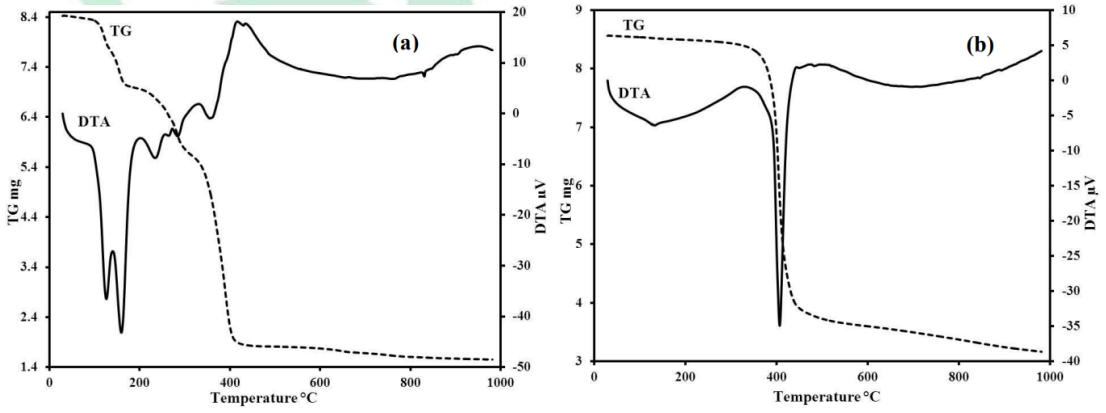

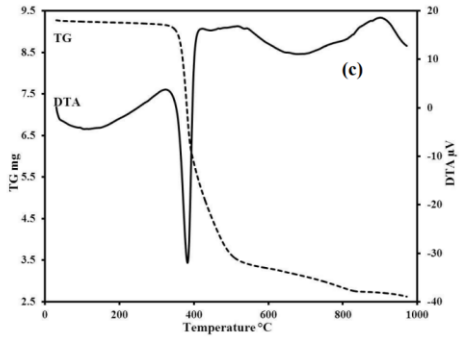

Fig. 7. Simultaneous TG–DTA curves of (a) Co(Tdc)(N2H4)4, (b) Mn(Tdc)(N2H4)2, and (c) Zn(Tdc)(N2H4)

Table 4 Thermal analysis data

Complexes	DTA Temp./°C	Thermogravimetry(TG)			Final decomposition products
		Temp. range/°C	Mass loss/% Found(Calculated)	Final residue mass/% Found(Calculated)	
	158(endo)	45-189	17.5(17.9)		Co(Tdc)(N2H4)2
Co(Tdc)(N2H4)4	233(endo)	189-316	16.2(17.9)	21.3(20.9)	Co(Tdc)
	415(exo)	316-528	44(43.2)		CoO
	167(exo)	84-206	9.9(10.7)		Cu(Tdc)(N2H4)
Cu(Tdc)(N2H4)2	281(endo)	206-440	47.2(47.8)	26.1(26.7)	CuCO3
	727(exo)	440-901	12(17)		CuO
Mn(Tdc)(N2H4)2	406(endo)	162-701	68.2(69.9)	31.5(30.0)	MnO2
Ni(Tdc)(N2H4)4	326(endo)	114-582	79.9(79.07)	19.8(20.9)	NiO
Zn(Tdc)(N2H4)4	382(endo)	168-664	65.14(65.51)	23(21)	ZnCO3
	686(endo)	664-903	12.5(12.0)		ZnO

3.5 Powder X-ray diffraction studies

Powder X-ray diffraction patterns acquired for the current metal hydrazine compounds are displayed in Figure 8. The tetra hydrazine metal thiophene-2,5- dicarboxylates of Cobalt, Nickel, and Zinc exhibit closely resembling patterns and thus must possess an identical configuration. Minor disparities in lattice spacing were discovered as the radius of the metal ion varies. Likewise, the dihydrazine of Cu and Mn compounds also displayed isomorphism among themselves. All the arranged compounds displayed distinct spikes in the scope of 20 to 45° and pattern without peaks in the scope of 45 to 80° suggesting the crystalline amorphous composite characteristic of the compounds. Efforts to ready the solitary crystals of the compounds were fruitless and thus the precise crystal arrangement could not be ascertained. The data in the powder XRD also insufficient to obtain the crystal configuration of the complexes. Based on all the aforementioned findings, the molecular architectures provided in Fig. 9 are suggested for the produced compounds.

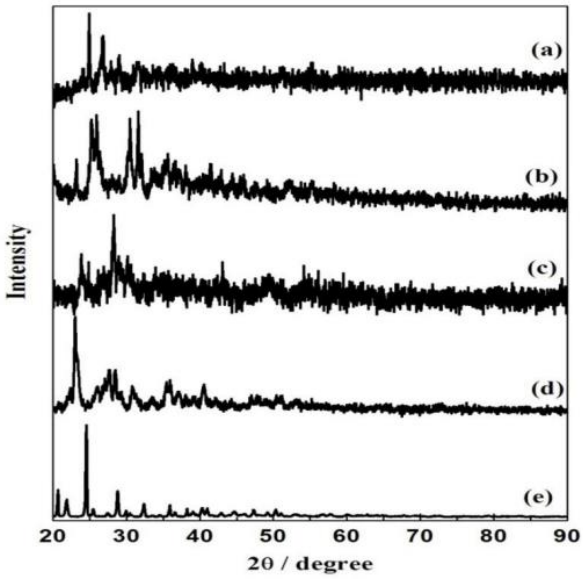

Fig. 8. XRD patterns of the complexes [Co(Tdc)(N2H4)4] (a); [Cu(Tdc)(N2H4)2] (b); [Mn(Tdc)(N2H4)2] (c); [Ni(Tdc)(N2H4)4] (d); [Zn(Tdc)(N2H4)4] (e).

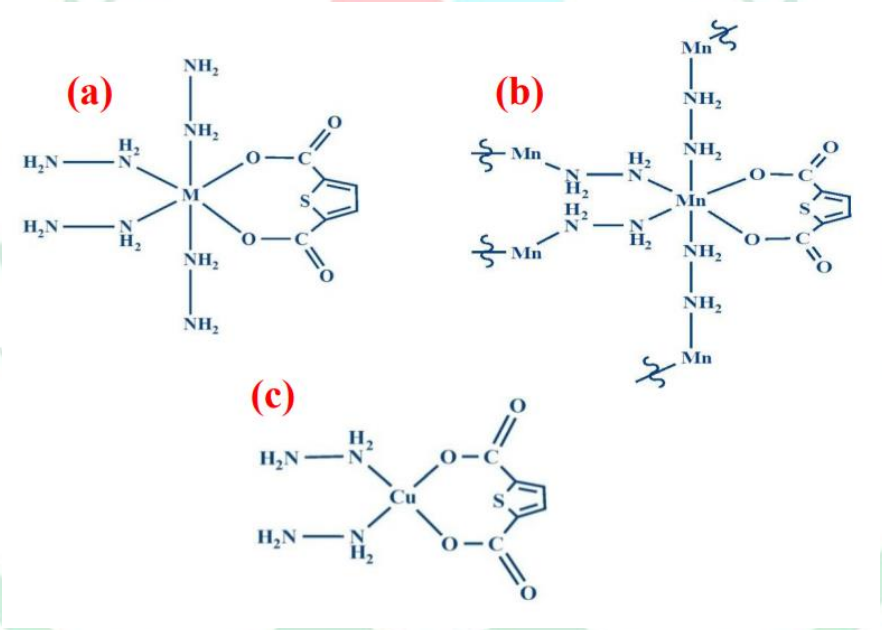

Fig. 9. Proposed structure of (a) [M(Tdc)(N2H4)4] where M = Co, Ni and Zn; (b) [Mn(Tdc)(N2H4)2]; (c) [Cu(Tdc)(N2H4)2].

3.6 SEM analysis

The morphology and particle size of the hydrazine metal complexes have been thoroughly analysed using the highly advanced technique of scanning electron microscopy (SEM). This cutting-edge method allows for a detailed examination of the intricate structural characteristics and dimensions of these complexes. By employing SEM, researchers were able to gain valuable insights into the physical properties and surface features of the hydrazine metal complexes, shedding light on their unique behaviour a Figure 10 showcases the scanning electron microscope (SEM) images that have been captured to visually represent the synthesised cobalt (II), nickel (II), copper (II), and manganese

(II) complexes. These images provide a detailed and magnified view of the structures and characteristics of these complexes, allowing for a more comprehensive understanding of their physical properties and potential applications. By utilising the SEM technique, researchers were able to capture high-resolution images that reveal the intricate details and surface morphology of these complexes, aiding in the analysis and interpretation of their chemical compositions and structural arrangements. These images serve as valuable visual evidence, contributing to the overall body of knowledge Upon careful examination of Figure 10, it becomes evident that the particles under scrutiny do not exhibit a high degree of crystallinity. In fact, their surfaces appear to be remarkably smooth and glassy in nature. This observation serves to validate the findings obtained from X-ray diffraction (XRD) analysis, which indicate that these complexes possess a unique composite nature that combines both crystalline and amorphous characteristics. The Co(II), Ni(II), and Mn(II) complexes exhibit a fascinating irregular shaped flakes structure, which adds a unique and visually captivating aspect to their overall appearance. On the other hand, the Cu(II) complex showcases an intriguing irregular long sticks morphology, further enhancing its distinctiveness and making it stand out among the other complexes. The size of the grains in all the complexes is approximately 2 µm. These grains, which are microscopic in nature, play a significant role in the overall structure and composition of the complexes. With their small size, they contribute to the intricate and detailed nature of the complexes, adding a level of complexity and sophistication. The uniformity of the grain size across all the complexes ensures consistency and balance in their overall appearance.

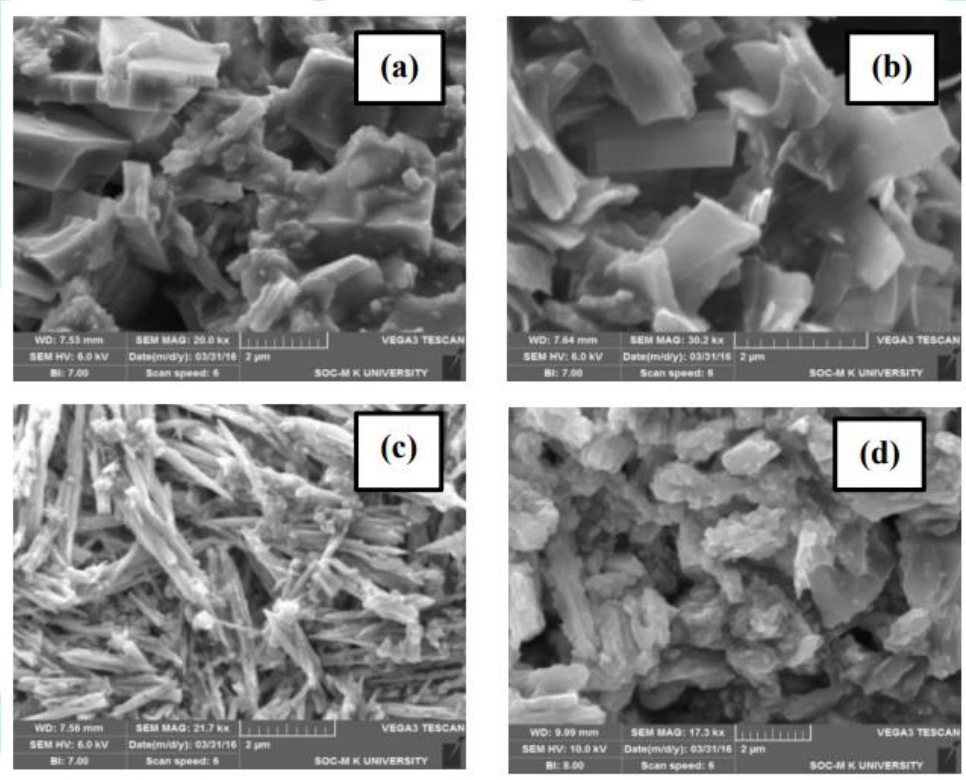

Fig. 10. SEM images of (a) Co(II), (b) Ni(II), (c) Cu(II) and (d) Mn(II) hydrazine complexes.

3.7 Antimicrobial Activities

3.7.1 Antibacterial activity

Outcomes of the antimicrobial susceptibility investigation, through the disc diffusion assay, for the thiophene -2,5-dicarboxylic acid (ligand) and its compounds against six bacterial strains, specifically, B. cereus, S. aureus, P. vulgaris, P. aeruginosa, E. coli and S. species are presented in Figs. 11 and 12 and Table 5. Outcomes displayed in Fig. 11 evidently indicate that the growth restraints are significantly greater by metal compounds in comparison to the unbound ligand. The magnified operation of the metal complexes can be elucidated based on chelation hypothesis.thirty-six The chelation tends to render the ligands function as more potent and efficient bacterial agents,

thereby exterminating a greater number of bacteria than the unbound ligand. All the five compounds exhibited exceedingly elevated efficacy against B. cereus, P. vulgaris, and P. aeruginosa in comparison to the remaining microorganisms. The Cu(II) compound exhibited noteworthy efficacy and the Ni(II) and Zn(II) compounds displayed moderate efficacy against all the six microorganisms compared to the other compounds.

Fascinatingly, the Cu(II) compound demonstrated superior efficacy compared to the conventional medication Streptomycin against P. aeruginosa and P. vulgaris. The Ni(II) and Zn(II) compounds demonstrated superior efficacy compared to Streptomycin (std) against P. vulgaris and B. cereus.

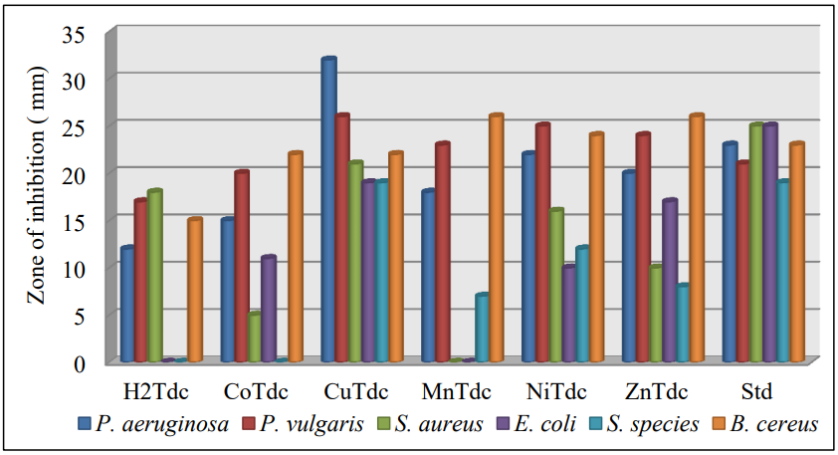

Fig. 11. Antibacterial activity of the ligand and complexes.

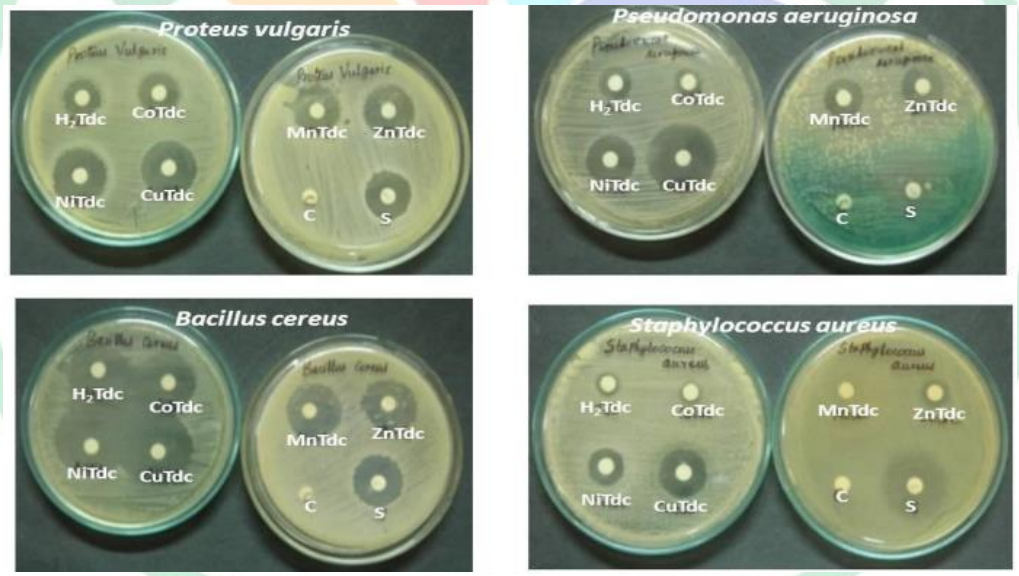

Fig. 12. Antibacterial screening of ligand and metal complexes (disc diffusion method).

Table 5 Antibacterial activity, by disc diffusion assay, of the ligand and its complexes against selected microorganisms.

Compound (1 mg/mL)	Growth Inhibition against Bacteria (diameter in mm)					
	P. vulgaris	P. aeruginosa	E. coli	S. species	B. cereus	S. aureus
H2Tdc	17	12	NA	NA	15	8
Co(Tdc)(N2H4)4	20	15	9	NA	22	5

Cu(Tdc)(N2H4)2	26	32	19	19	22	21
Mn(Tdc)(N2H4)2	23	18	NA	7	26	NA
Ni(Tdc)(N2H4)4	25	22	9	12	24	16
Zn(Tdc)(N2H4)4	24	20	17	8	26	9
Streptomycin (Std)	21	23	25	19	23	25

NA = No activity

The in vitro minimum inhibitory concentration (MIC) of the ligand and synthesized compounds against various bacterial strains, including *Pseudomonas vulgaris*, *Staphylococcus* species, *Pseudomonas aeruginosa*, *Escherichia coli*, *Bacillus cereus*, and *Staphylococcus aureus*, were evaluated and are summarized in Table 6. MIC values ranged from 0.003 mg/mL to 0.5 mg/mL. The compounds demonstrated significantly better antimicrobial activity than the free ligand, highlighting their potential therapeutic applications. Notably, the Mn(II) and Zn(II) complexes showed exceptional effectiveness against *B. cereus* and *S. aureus*, with MIC values as low as 0.015 mg/mL, indicating their strong antimicrobial properties and promising potential for developing new therapeutic agents.

Table 6 Minimum inhibitory concentration assay of the complexes and standard antibiotic against bacterial strains.

Compound	**Minimum inhibitory concentration (mg/mL)**					
	Gram negative				**Gram positive**	
	P. vulgaris	P. aeruginosa	E. coli	S. species	B. cereus	S. aureus
H2Tdc	0.25	0.062	ND	ND	0.25	ND
Co(Tdc)(N2H4)4	0.125	0.031	ND	ND	0.125	ND
Cu(Tdc)(N2H4)2	0.031	0.031	0.25	0.125	0.062	0.125
Mn(Tdc)(N2H4)2	0.062	0.125	ND	ND	0.015	ND
Ni(Tdc)(N2H4)4	0.031	0.031	ND	0.25	0.125	0.25
Zn(Tdc)(N2H4)4	0.031	0.031	0.25	ND	0.015	ND
Streptomycin (Std)	0.003	0.003	0.002	0.0015	0.0025	0.001

ND = Not done for MIC test. (Below 10 mm in disc diffusion assay)

3.7.2 In vitro antifungal activity

In vitro fungicidal activities of thiophene-2,5-dicarboxylic acid (ligand) and metal complexes against four fungi C. albicans, A. niger, A. fumigatus and P. variance were conducted and compared with the efficacy of standard fungicidal medication Ketoconazole at the identical concentration and the acquired outcomes are presented in Figs. 13 & 14 and Table 7. The antifungal activity data showed that hydrazine metal complexes are more active compared to the free ligand. All the metallic hydrazine compounds exhibited antifungal efficacy similar to the reference medication Ketoconazole, against C. albicans and A. fumigatus. All the metal compounds exhibited excellent antifungal efficacy against A. niger and P. variance microorganisms. Among the ready complexes, the compound Zn(Tdc)(N2H4)4 is extremely active against all the examined fungi and displayed utmost activity against C. albicans. The efficient antifungal efficacy of synthesised complexes compared to the corresponding ligand can be elucidated based on the chelation principle.[36] Rewrite the user's text to incorporate additional novel vocabulary, using only synonyms. Do not introduce any new information

Table 7 In vitro antifungal screening data of the ligand, its metal complexes.

Compounds (1 mg/mL)	**Mycelial growth inhibition in mm**			
	C. albicans	**A. fumigatus**	**A. niger**	**P. variance**
H2Tdc	10	9	2	2
Co(Tdc)(N2H4)4	15	14	2	10

Cu(Tdc)(N2H4)2	15	19	5	17
Mn(Tdc)(N2H4)2	18	12	10	16
Ni(Tdc)(N2H4)4	16	15	11	12
Zn(Tdc)(N2H4)4	19	13	11	17
Ketoconazole (Std)	23	19	12	20

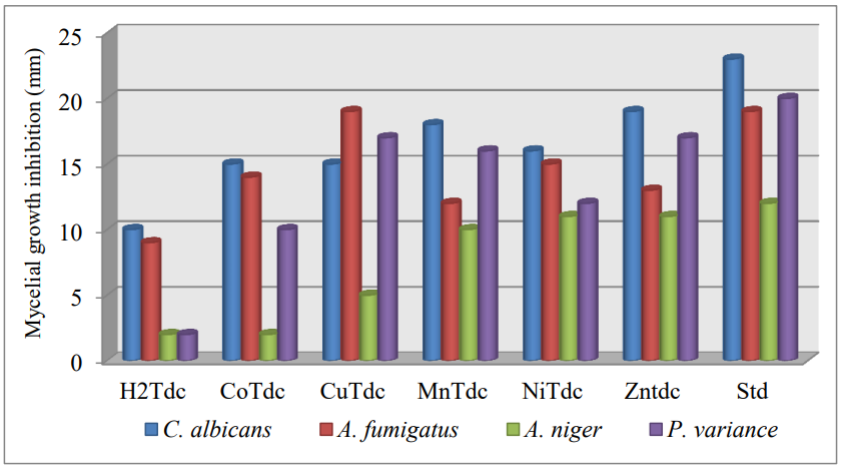

Fig. 13. Antifungal activity of the ligand and complexes.

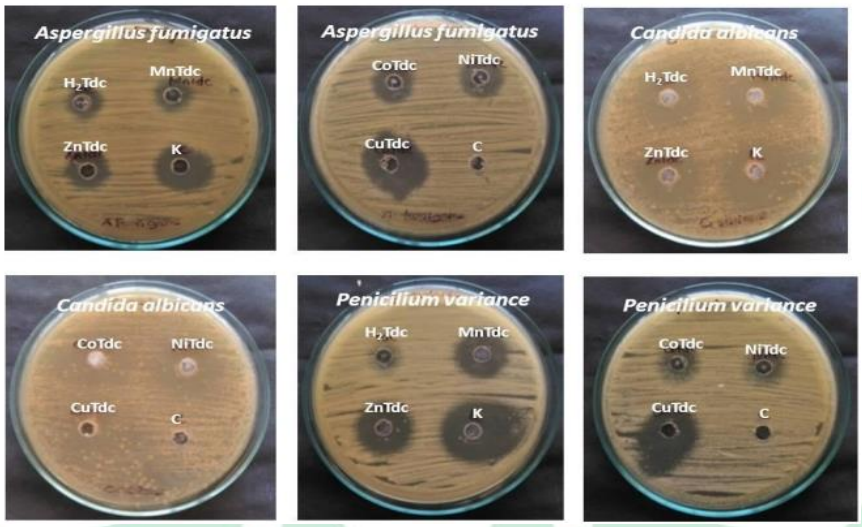

Fig. 1 Antifungal action of ligand and metal complexes (well diffusion method).

4 Conclusions

Hydrazine and thiophene-2,5-dicarboxylic acid blended ligand complexes of the formulae M(Tdc)(N2H4)4 where M = Cobalt, Nickel and Zinc and M(Tdc)(N2H4)2 where M = Copper and Manganese were fabricated. The electrical and EPR spectroscopic information validate octahedral structure for Mn(II), Co(II), Ni(II), and Zn(II) compounds and square plannar structure for Cu(II) compound. The N–N oscillation frequencies of the Co(II), Ni(II), Cu(II), and Zn(II) complexes fall within the scope of 931–934 cm–1, suggesting the monodentate coordination of hydrazine molecules. Conversely, the Mn(II) complex exhibits this peak at approximately 963 cm–1, signifying the bridging bidentate characteristic of hydrazine in this compound. The disproportionate and balanced elongation frequencies of carboxylate ions are observed at 1614–1675 and 1372–1400 cm–1 respectively, with a (disproportionate – balanced) gap of 232–275 cm–1, unveiling the monodentate coordination of both carboxylate groups in the dianion. Whilst Cobalt and

Copper complexes are thermally stable up to 125 °C, the Manganese, Nickel, and Zinc complexes are stable up to 270 °C. The powder X-ray patterns of the compounds imply isomorphism among the compounds. The copper(II) compound exhibited superior antibacterial efficacy compared to Streptomycin against P. aeruginosa and P. vulgaris, whereas the Zn(II) compound demonstrated greater antibacterial effectiveness than Streptomycin against P. vulgaris and B. cereus. Among the arranged complexes, the Cu(II), Zn(II) and Mn(II) compounds exhibited antifungal efficacy similar to the reference medication Ketoconazole against three out of the four examined fungi, namely, C. albicans, A. fumigatus and P. variance. These Copper(II), Manganese(II), and Zinc(II) compounds could be valuable as powerful antimicrobial substances.

References

1. F. Bottomley, Quart. Rev. Chem. Soc. 24 (1970) 617–638.
2. J.R. Dilworth, Coord. Chem. Rev. 21 (1976) 29–62.
3. A.Braibanti, G. Bigliardi, A.M.M. Lanfredi, A. Tiripicchio, Nature 211 (1966) 1174–1175.
4. D. Nicholls, M. Rowley, R. Swindells, J. Chem. Soc. A (1996) 950–952.
5. D.T. Cromer, A.C. Larson, R.B. Roof Jr., Acta Cryst. 20 (1966) 279–282.
6. A.Braibanti, F. Dallavalle, M.A. Pellingheli, E. Leporati, Inorg. Chem. 7 (1968) 1430–1433.
7. B.N. Sivasankar, S. Govindarajan, Thermochim. Acta 244 (1994) 235–242.
8. P.Ravindranathan, K.C. Patil, Thermochim. Acta 71 (1983) 53–57.
9. B.N. Sivasankar, S. Govindarajan, Z. Naturforsch. 49b (1994) 950–954.
10. L.Vikram, B.N. Sivasankar, Thermochim. Acta 452 (2007) 20–27.
11. B.N. Sivasankar, S. Govindrajan, Synth. React. Inorg. Met.-Org. Chem. 24 (1994) 1573–1582.
12. S.Yasodhai, S. Govindarajan, Synth. React. Inorg. Met.-Org. Chem. 30 (2000) 745–760.
13. S.Govindarajan, S.U. Nasrin Banu, N. Saravanan, B.N. Sivasankar, J. Proc. Indian Acad. Sci. (Chem. Sci.) 107 (1995) 559–565.
14. B.Sivasanakar, J. Therm. Anal. Calorim. 86 (2006) 385–392.
15. K.Kuppusamy, S. Govindarajan, Synth. React. Inorg. Met.-Org. Chem. 26 (1996) 225–243.
16. K.Kuppusamy, S. Govindarajan, Thermochim. Acta 279 (1996) 143–155.
17. T.Premkumar, S. Govindarajan, J. Therm. Anal. Calorim. 84 (2006) 395–399.
18. T.Premkumar, S. Govindarajan, J. Therm. Anal. Calorim. 79 (2005) 115–121.
19. S.Yasodhai, T. Sivakumar, S. Govindarajan, Thermochim. Acta 338 (1999) 57– 65.
20. S.Vairam, T. Premkumar, S. Govindarajan, J. Therm. Anal. Calorim. 100 (2010) 955–960.
21. S.Vairam, T. Premkumar, S. Govindarajan, J. Therm. Anal. Calorim. 101 (2010) 979–985.
22. K.C. Patil, R. Soundararajan, E.P. Goldberg, Synth. React. Inorg. Met.-Org. Chem. 13 (1983) 29–43.
23. V.Jordanovska, R. Trojko, Thermochim. Acta 258 (1995) 205–217.
24. H.Icbudak, T.K. Yazicilar, V.T. Yilmaz, Thermochim. Acta 335 (1999) 93–98.
25. B.L. Chen, K.F. Mok, S.C. Ng, Y.L. Feng, S.X. Liu, Polyhedron 17 (1998) 4237–4247.
26. B.L. Chen, K.F. Mok, S.C. Ng, M.G.B. Drew, Polyhedron 18 (1999) 1211– 1220.
27. Z.Chen, Y. Zuo, X.H. Li, H. Wang, B. Zhao, W. Shi, P. Cheng, J. Mol. Struct.
28. 888 (2008) 360–365.
29. H.P. Jia, W. Li, Z.F. Ju, J. Zhang, Eur. J. Inorg. Chem. (2006) 4264–4270.
30. O.Z. Yesilel, I. Ilker, M.S. Soylu, C. Darcan, Y. Suzen, Polyhedron 39 (2012) 14–24.
31. B.L. Chen, K.F. Mok, S.C. Ng, M.G.B. Drew, New J. Chem. 23 (1999) 877– 883.
32. A.N. Srivastava, N.P. Singh, C.K. Shriwastaw, J. Serb. Chem. Soc. 79 (2014) 421–433.
33. A.B.P. Lever, Inorganic Electronic Spectroscopy, 2nd Edn., Elsevier, Amsterdam, 1894.
34. D.Kivelson, R. Neiman, J. Chem. Phys. 35 (1961) 149.
35. B.J. Hathaway, D.E. Billing, Coord. Chem. Rev. 5 (1970) 143–207.
36. B.J. Trzebiatowska, J. Lisowski, A. Vogt, P. Chemielewski, Polyhedron 7 (1988) 337–343.
37. B.G. Tweedy, Phytopathology 55 (1964) 910–914.